Supporting Information

Overlooked intensity-effect relationship beyond dose-effect relationship in bacteria disinfection by 254 nm ultraviolet light

Si-Yi Shi[a], Lei Chen[a], Jian Zhao[b], Li Li[b], Hai-Sheng Du[c], Jun-Jie Wang[a], Wei Hu[d], Ye Du[a,*]

[a]College of Architecture and Environment, Sichuan University, Chengdu 610000, China

[b]Chengdu Xingrong Environment Co., Ltd., Chengdu 610095, China

[c]Sichuan Macyouwei Environmental Protection Technology Co., Ltd, Chengdu 610000, China

[d]Department of Civil and Environmental Engineering, University of Alberta, Edmonton, AB T6G 1H9, Canada

Corresponding author:

Ye Du

Add: College of the Architecture and Environment, Sichuan University, Chengdu 610065, China

Email: duyeah@scu.edu.cn

Number of pages: 21

Number of figures: 8

Number of tables: 4

Text S1 Chemicals and reagents

Potassium iodide (KI, analytical reagent, Kelong Chemical Co., Chengdu, China), sodium tetraborate decahydrate ($Na_2B_4O_7 \cdot 10H_2O$, analytical reagent, Shanghai Macklin Biochemical Co., Ltd., Shanghai, China) and potassium iodate (KIO_3, analytical reagent, Shanghai Macklin Biochemical Co., Ltd) were used to prepare KI/ KIO_3 actinometer stock solution.

Strains of Escherichia coli (*E. coli*) were purchased from Tsingke Biological Technology (Beijing, China). *Bacillus subtilis* (*B. subtilis*) strains were purchased from the China General Microbiological Culture Collection Center (Beijing, China). Luria–Bertani broth and Luria–Bertani nutrient agar were purchased from Beijing Aoboxing Biology Technology (Beijing, China). Fuchsine basic sodium sulfite agar (Qingdao Hope BioTechnology Co., Qingdao, China) was used to detect *E. coli* in actual wastewater.

Sodium chloride (NaCl, analytical reagent, Cologne Chemical Co., LTD.) is dissolved in ultra-pure water to prepare normal saline with a concentration of 0.9%. Phosphate-buffered saline was purchased from Shanghai Zhong Qiao Xin Zhou Biotechnology (Shanghai, China). 5, 5-dimethyl-1-pyrrolin-n-oxide (DMPO), 2, 2,6, 6-tetramethylpiperidine (TMP), tert-butanol and L-histidine were purchased from Aladdin Chemical (Shanghai, China). Live/dead BBcellProbe N01/ PI bacterial viability kits were purchased from BestBio (Shanghai, China).

Text S2 Preparation and counting of *Escherichia coli* and *Bacillus subtilis*

Escherichia coli (*E. coli*) and *Bacillus subtilis* (*B. subtilis*) strains were preserved in glycerol stocks and stored at -80 °C. Under sterile conditions, frozen *E. coli* or Bacillus subtilis cultures were thawed in water at 37 °C. Using a pipette, 50 μL of the bacterial suspension was transferred to 200 mL of autoclaved LB nutrient broth. The mixture was then incubated with shaking at 160 rpm and 37 °C. *E. coli* was incubated for 18 hours, while Bacillus subtilis was incubated for 48 hours. After incubation, the culture broth was centrifuged at 4800 rpm for 5 minutes. The supernatant was discarded, and the pellet was resuspended in a specified volume of sterile normal saline and mixed thoroughly. This process was repeated twice. The precipitate was re-suspended in the brine, and the resulting mixture was analyzed using an ultraviolet spectrophotometer (INESA, China). The mixture was diluted to an initial cell concentration of approximately 10^6 to 10^8 CFU/mL.

Bacteria were quantified using the dilution plating method (Pezeshkpour et al., 2018). Specifically, 50 μL of appropriately diluted water samples were evenly spread on the surface of LB agar plates using sterile L-shaped spreaders. Each dilution gradient included three replicate samples. The plates were incubated upside down at 37 °C for 24 hours. Plates containing between 30 and 300 colonies were selected for enumeration, and the average colony count was calculated.

Text S3 Microwave discharge electroless ultraviolet disinfection device

In this study, a quasi-parallel beam instrument was constructed using microwave

discharge electrodeless lamps (MDEL), as illustrated in Figure S1. Although microwave-driven, the MDEL confines microwaves internally and produces no ozone, ensuring that disinfection arises solely from UV irradiation at varying intensities. The apparatus is composed of an outer shell, radiator, and connecting pipe. A lifting platform and magnetic stirrer are positioned beneath the parallel tube, enabling vertical adjustment of the reaction vessel relative to the UV lamp to precisely control light intensity. The lifting platform facilitates fine-tuning of the distance between the UV source and the reaction solution surface, allowing accurate setting of the desired UV intensity across experimental conditions. Continuous operation of the magnetic stirrer ensures homogeneous mixing of the reaction solution, preventing localized concentration gradients and promoting consistent UV exposure.

The MDEL system emits UV light with a peak wavelength of 254 nm and a maximum output power of over 20 mW/cm^2 at close range. UV intensity at the reaction surface was measured and calibrated using the KI/KIO_3 chemical actinometer method (Bolton and Linden, 2003) to ensure accuracy and stability throughout the experiments. Measurements confirmed that UV intensity was stable over the experimental duration. The dose consistency was maintained by applying the corresponding exposure time at each light intensity level, calculated as the product of intensity and time.

Text S4 Inactivation and photoreactivation analysis methods

The Chick–Watson first-order kinetic model was utilized to characterize the disinfection process (Hijnen et al., 2006). The inactivation rate constant and bacterial

inactivation efficiency were calculated using Equation (1) to assess disinfection performance：

$$\text{Inactivation rate}=\log(N_0/N) = K_d \times D \quad (1)$$

Where K_d is the inactivation rate constant (cm^2/mJ), and D signifies the UV dose (mJ/cm^2).

The photoreactivation characteristics of *E. coli* were assessed using the photoreactivation rate and a photoreactivation model. The maximum reactivation value, defined as the bacterial count (CFU/mL) after complete photoreactivation of *E. coli*, was determined. The photoreactivation rate was calculated using Eq. (2) (Lindenauer and Darby, 1994):

$$\text{photoreactivation rate}= (N_t\text{-}N)/(N_0\text{-}N) \times 100\% \quad (2)$$

Where N_0 represents the initial bacterial count before disinfection (CFU/mL), N denotes the bacterial count after ultraviolet irradiation (CFU/mL), and N_t indicates the bacterial count after photoreactivation (CFU/mL).

The photoreactivation process of microorganisms can be described in terms of survival rate, which is independent of the initial bacterial count. The survival rate (S) was calculated using Eq. (3) (Kashimada et al., 1996):

$$S= N_t/N_0 \times 100\% \quad (3)$$

The photoreactivation process of microorganisms was modeled using a logistic regression equation, as shown in Eq. (4) (Nebot Sanz et al., 2007):

$$S= S_m/\left[1+(S_m/S_0 - 1)\times e^{-k_2 \cdot S_m \cdot t}\right] \quad (4)$$

Where Sm represents the maximum survival rate (%), S_0 denotes the survival

rate after disinfection (%), and k_2 signifies the secondary reactivation rate constant ($\%^{-1}h^{-1}$).

The model parameters in this model are utilized for predicting experimental outcomes rather than representing the actual reactivation rate constant. The light reactivation rate constant was recalculated using Eq. (5) (Li et al., 2017):

$$K = ds/dt = k_2(S_m\text{-}S)S \quad (5)$$

The maximum reactivation rate constant, K_{max}, was determined using Eq. (6), where the survival rate reaches 50% of the maximum survival rate and the reactivation rate K attains its peak value:

$$K_{max} = k_2 {S_m}^2/4 \quad (6)$$

In this study, a logistic regression model was employed to fit the photoreactivation process. The model parameter k_2 was estimated and compared with K_{max}. Specifically, S_m denotes the maximum survival rate of bacteria following reactivation, which indicates the extent of photoreactivation, while K_{max} represents the maximum reactivation rate of bacteria.

Text S5 RNA sequencing and bioinformatics analysis

The collected cell pellets were transferred to RNA-free cryotubes and rapidly frozen in liquid nitrogen for 30 minutes prior to extraction. RNA sequencing was performed by Majorbio Co. Ltd., China. Total RNA extraction was conducted using TRIzol® reagent (R0016, Beyotime, China), followed by genomic DNA removal with DNase I (TaKara, Japan). The Ribo-Zero magnetic kit (Epicenter Biotechnologies, WI,

USA) was used to deplete 16S and 23S ribosomal RNA (rRNA) from the total RNA. Subsequently, the mRNA was fragmented into approximately 200 bp segments using a fragmentation buffer. Double-stranded cDNA was synthesized from these fragments using the SuperScript double-stranded cDNA synthesis kit (Invitrogen, CA) and random hexamer primers (Illumina, USA). Incorporation of deoxyuridine triphosphate (dUTP) in place of deoxythymidine triphosphate (dTTP) during second-strand synthesis resulted in the generation of blunt-ended cDNA.Double-stranded cDNA undergoes sequential processing steps including terminal repair, phosphorylation, 3' adenylation, and adapter ligation. Subsequently, the second strand of cDNA, which incorporates dUTP, is degraded using uracil-N-glycosylase (UNG). The resulting cDNA fragments are separated on a 2% agarose gel, from which DNA fragments approximately 200 bp in length are excised and used as templates for constructing the cDNA library. The library is amplified via PCR using Phusion DNA polymerase (NEB, USA) for a total of 15 cycles. Following quantification with a microfluorimeter (TMS-380, TurnerBioSystems, USA), the library is subjected to paired-end sequencing on the Illumina HiSeq X Ten platform.

Text S6 EPR analysis of reactive oxygen species

Electron paramagnetic resonance (EPR) analysis was conducted to detect the production of hydroxyl radicals (•OH) and singlet oxygen ($^1O_2$) induced by 254 nm UV irradiation at varying intensities. A 10 mL water sample was prepared by adding 50 μL of the spin trap agent, either 5,5-dimethyl-1-pyrroline-N-oxide (DMPO) for

•OH detection or 2,2,6,6-tetramethylpiperidine (TEMP) for $^1O_2$ detection, prior to UV irradiation. Samples were then exposed to UV light at different intensities (1, 5, and 10 mW/cm^2) for corresponding durations to achieve an identical UV dose of 20 mJ/cm^2 across all conditions.

Immediately after irradiation, a small volume of the reaction mixture was drawn into a capillary tube and subjected to EPR analysis using a Bruker EMXplus X-band spectrometer (Germany) under the following settings: microwave frequency 9.86 GHz, power 2.00 mW, modulation frequency 100.00 kHz, modulation amplitude 1.0 G. Each EPR spectrum was obtained by averaging five scans to improve signal clarity. The experimental conditions, including UV dose and exposure time, were kept consistent for all samples to ensure comparability between different intensity levels.

Table S1 Evaluation of model fitting parameters and statistical indicators for bacterial inactivation.

Bacterial Species	k'/ln10 ±SE[a]	n±SE	RMSE[b]	Reduced Chi-Sqr[c]	R^2	F[d]	p-value[e]
E. coli	0.22 ±0.013	1.37 ±0.040	0.22	0.89	0.96	398.13	<0.0001
B. subtilis	0.14 ±0.009	1.28 ±0.038	0.18	0.95	0.92	359.22	<0.0001
Fecal coliforms	0.13 ±0.014	1.68 ±0.072	0.19	0.85	0.91	297.13	<0.0001

Note:

[a] Standard error (SE) indicates the variability or precision of the estimated parameter in the model fitting.

[b] Root mean square error (RMSE) measures the average magnitude of the residuals between observed and predicted values, reflecting the overall fitting accuracy.

[c] Reduced chi-square quantifies the goodness-of-fit of the model, with values closer to 1 indicating a better fit relative to data variability.

[d] F-test value assesses the overall significance of the model, comparing model variance to residual variance, where larger values indicate a stronger model fit.

[e] p-value indicates the probability of obtaining the observed results if the null hypothesis is true. A smaller p-value (e.g., < 0.05) suggests a stronger statistical significance of the model fit.

Table S2 Model parameters (S_m, k_2) and resurgence rate constants (K_{max}) for the photoreactivation of *E. coli* after 8.0 log disinfection.

MWUV intensity (mW/cm^2)	Observed S_m[a] (%)	Model S_m (%)	K_{max}[b] ($\%h^{-1}$)	k_2[c] ($\%^{-1}h^{-1}$)
1	0.1595	0.1702	0.1897	29.8195
2	0.0063	0.0064	0.0051	509.9467
5	0.0011	0.0008	0.0007	2183.3077
10	0.0001	0.0001	0.0000	9953.2500

Note:

[a] S_m means the maximum survival rate after the bacterial resurrection and represents the degree of photoreactivation.

[b] K_{max} means the maximum value of bacterial resurrection rate and represents the rate of resurrection.

[c] k_2 means the secondary resurgence rate constant and the Logistic Regression model parameter.

Table S3 Model parameters (S_m, k_2) and resurgence rate constants (K_{max}) for the photoreactivation of *B. subtilis* after 3.0 log disinfection.

MWUV intensity (mW/cm^2)	Observed S_m[a] (%)	Model S_m (%)	K_{max}[b] ($\%h^{-1}$)	k_2[c] ($\%^{-1}h^{-1}$)
1	3.2359	2.9811	1.6440	0.6280
2	1.6596	1.6570	0.8155	1.1843
5	1.0471	1.0328	0.2035	3.1346
10	0.4759	0.4764	0.1018	12.6663

Note:

[a] S_m means the maximum survival rate after the bacterial resurrection and represents the degree of photoreactivation.

[b] K_{max} means the maximum value of bacterial resurrection rate and represents the rate of resurrection.

[c] k_2 means the secondary resurgence rate constant and the Logistic Regression model parameter.

Table S4 Model parameters (S_m, k_2) and resurgence rate constants (K_{max}) for the photoreactivation of fecal coliform after 4.5 log disinfection.

MWUV intensity (mW/cm^2)	Observed S_m[a] (%)	Model S_m (%)	K_{max}[b] ($\%h^{-1}$)	k_2[c] ($\%^{-1}h^{-1}$)
1	10.2329	10.3245	12.5005	0.4775
2	3.2359	3.0172	1.7724	0.6771
5	0.4266	0.4391	0.1966	4.3225
10	0.0058	0.0049	0.0012	138.9121

Note:

[a] S_m means the maximum survival rate after the bacterial resurrection and represents the degree of photoreactivation.

[b] K_{max} means the maximum value of bacterial resurrection rate and represents the rate of resurrection.

[c] k_2 means the secondary resurgence rate constant and the Logistic Regression model parameter.

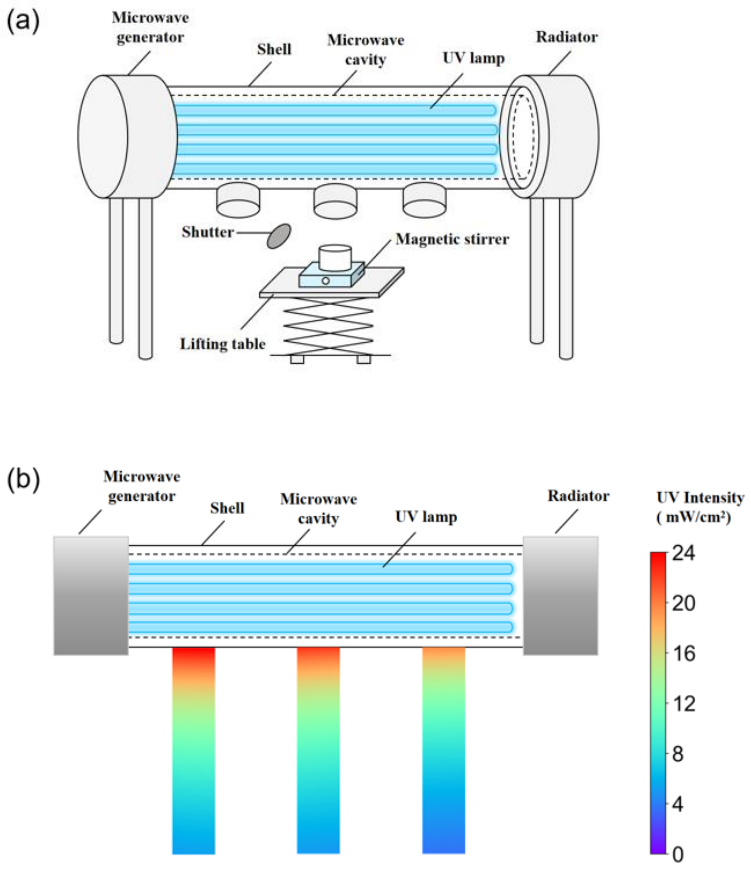

Figure S1 Schematic diagram of the UV experimental setup: (a) Schematic diagram of the quasi-parallel beam instrument based on MDEL; (b) Light field distribution diagram of MDEL.

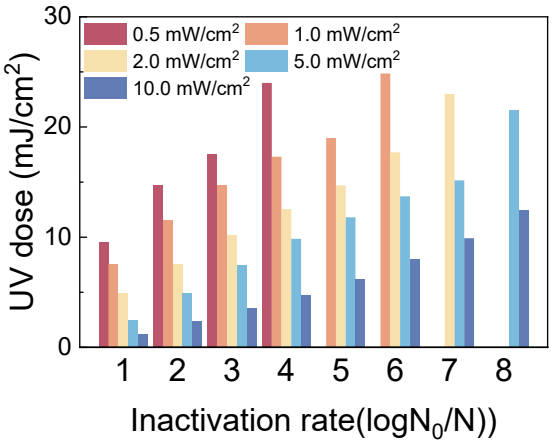

Figure S2 Required UV dose to achieve the target inactivation rate under different UV intensities

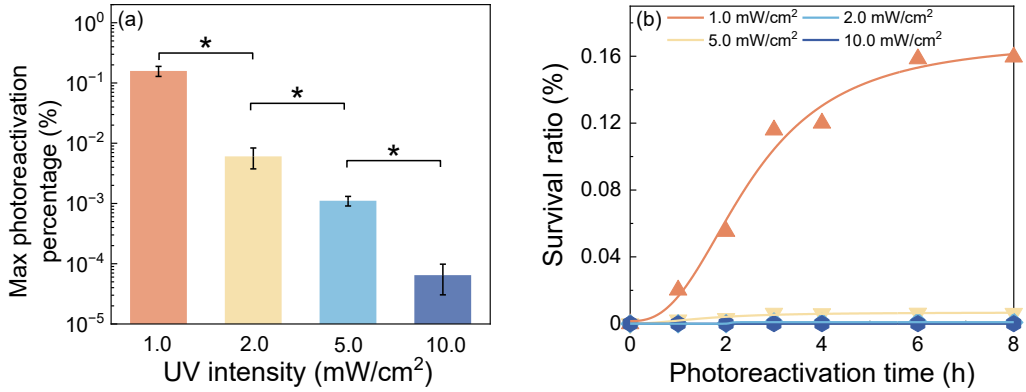

Figure S3 Reactivation characteristics of *E. coli* under different UV intensities after 8.0 log inactivation: (a) Maximum photoreactivation rates; (b) Photoreactivation model fitting (* indicates significant difference (p < 0.05) (one-way ANOVA)).

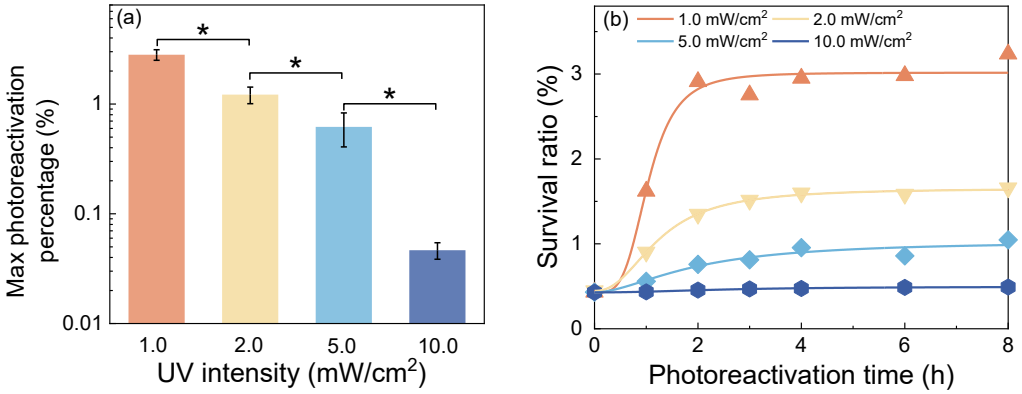

Figure S4 Reactivation characteristics of *B. subtilis* under different UV intensities after 3.0 log inactivation: (a) Maximum photoreactivation rates; (b) Photoreactivation model fitting (* indicates significant difference (p < 0.05) (one-way ANOVA)).

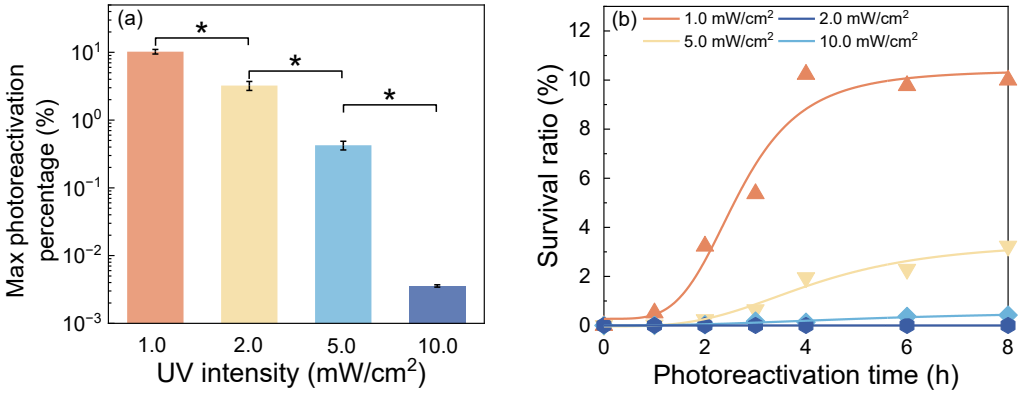

Figure S5 Reactivation characteristics of fecal coliform under different UV intensities after 4.5 log inactivation: (a) Maximum photoreactivation rates; (b) Photoreactivation model fitting (* indicates significant difference (p < 0.05) (one-way ANOVA)).

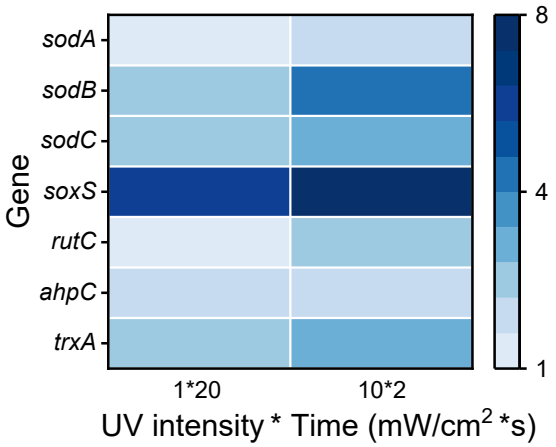

Figure S6 Key genes of ROS production and oxidative stress. Log_2 fold changes of relatively expression level compared with blank group.

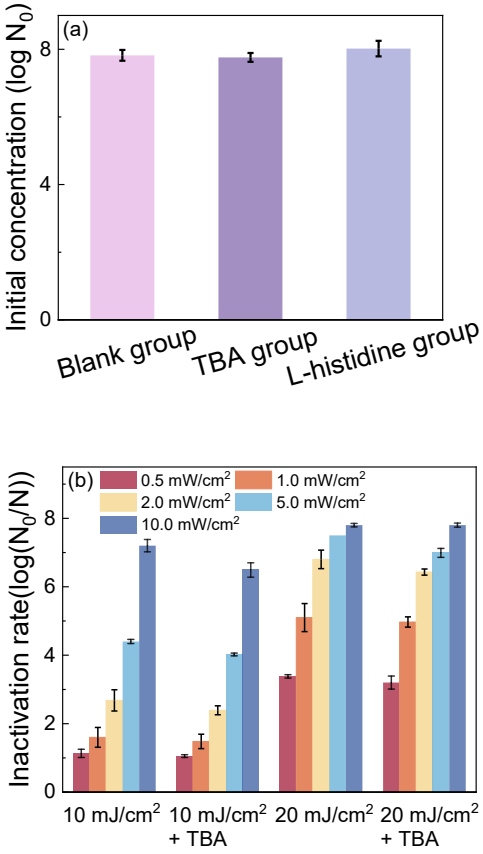

Figure S7 Inactivation of *E. coli* after shielding experiments: (a) The blank group, TBA group and L-histidine group were compared to confirm that the quenching agent itself did not affect the initial concentration of bacteria; (b) Effect of Singlet oxygen ($^1O_2$) on the inactivation of *E .coli* under different UV doses.

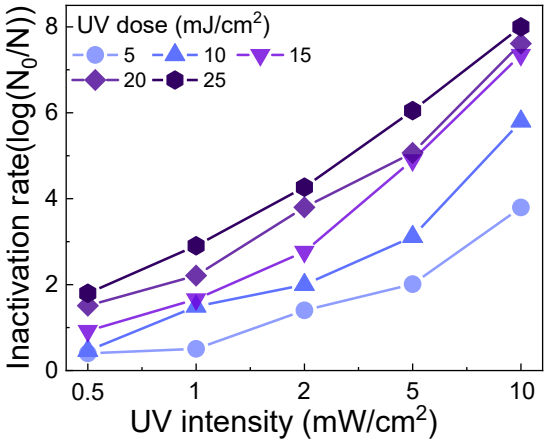

Figure S8 Trend of inactivation rate of *E. coli* with light intensity after quenching $^1O_2$.

References

Bolton, J.R., Linden, K.G., 2003. Standardization of methods for fluence (UV dose) determination in bench-scale UV experiments. J. Environ. Eng. 129, 209–215.

Hijnen, W.A.M., Beerendonk, E.F., Medema, G.J., 2006. Inactivation credit of UV radiation for viruses, bacteria and protozoan (oo)cysts in water: A review. Water Res. 40, 3–22.

Kashimada, K., Kamiko, N., Yamamoto, K., Ohgaki, S., 1996. Assessment of photoreactivation following ultraviolet light disinfection. Water Sci. Technol., Wastewater Reclamation and Reuse 1995 33, 261–269.

Li, G.-Q., Wang, W.-L., Huo, Z.-Y., Lu, Y., Hu, H.-Y., 2017. Comparison of UV-LED and low pressure UV for water disinfection: photoreactivation and dark repair of *escherichia coli*. Water Res. 126, 134–143.

Lindenauer, K.G., Darby, J.L., 1994. Ultraviolet disinfection of wastewater: Effect of dose on subsequent photoreactivation. Water Res. 28, 805–817.

Nebot Sanz, E., Salcedo Dávila, I., Andrade Balao, J.A., Quiroga Alonso, J.M., 2007. Modelling of reactivation after UV disinfection: effect of UV-C dose on subsequent photoreactivation and dark repair. Water Res. 41, 3141–3151.

Pezeshkpour, V., Khosravani, S.A., Ghaedi, M., Dashtian, K., Zare, F., Sharifi, A., Jannesar, R., Zoladl, M., 2018. Ultrasound assisted extraction of phenolic acids from *broccoli* vegetable and using sonochemistry for preparation of MOF-5 nanocubes: Comparative study based on micro-dilution broth and plate count method for synergism antibacterial effect. Ultrason. Sonochem. 40, 1031–1038.